Electronic Supplementary Information

Supramolecular assembly of dendronized spiropyrans in aqueous solutions into nanospheres with photo- and thermo- responsive chiralities

Shanbin Qi, Xueting Lu, Wenli Mei, Guanglei Gu, Wen Li* and Afang Zhang*

International Joint Laboratory of Biomimetic and Smart Polymers, School of Materials Science and Engineering, Shanghai University, Nanchen Street 333, Shanghai 200444, China

Table of Contents

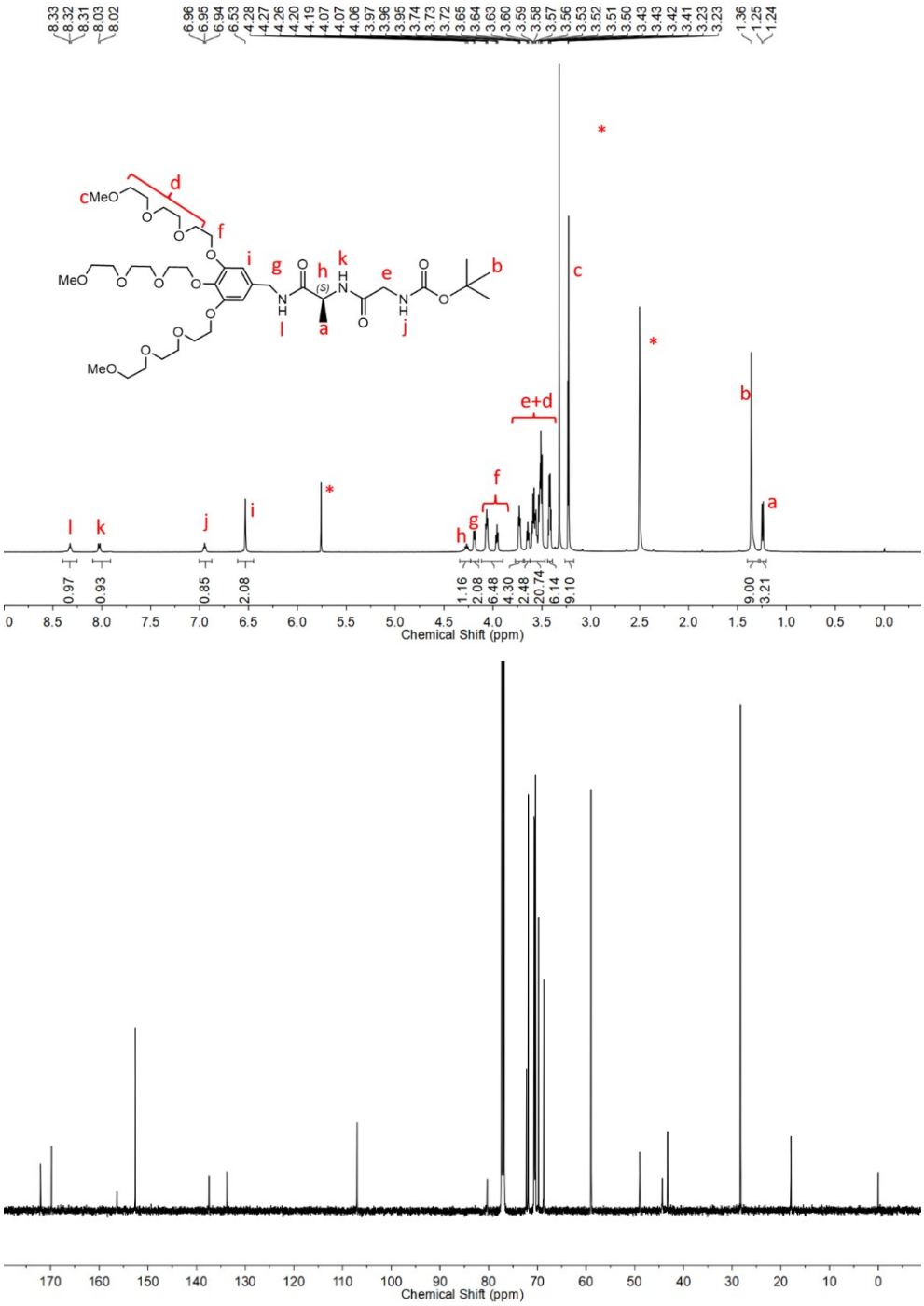

Fig. S1 ^{1}H (DMSO-d_6) and ^{13}C ($CDCl_3$) NMR spectrum of compound **2a** at 295 K.

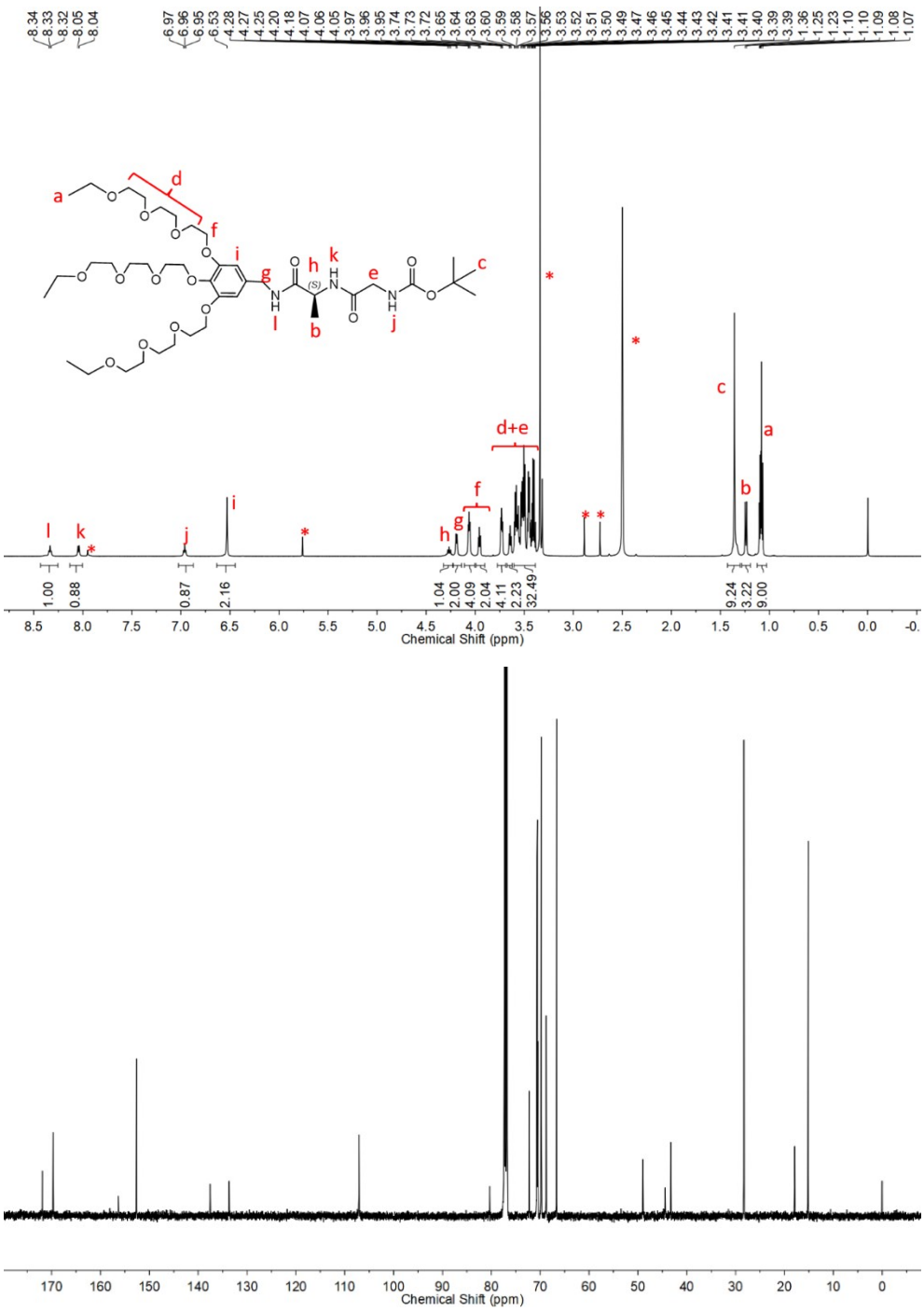

Fig. S2 ^{1}H (DMSO-d*6*) and ^{13}C ($CDCl_3$) NMR spectrum of compound **2c** at 295 K.

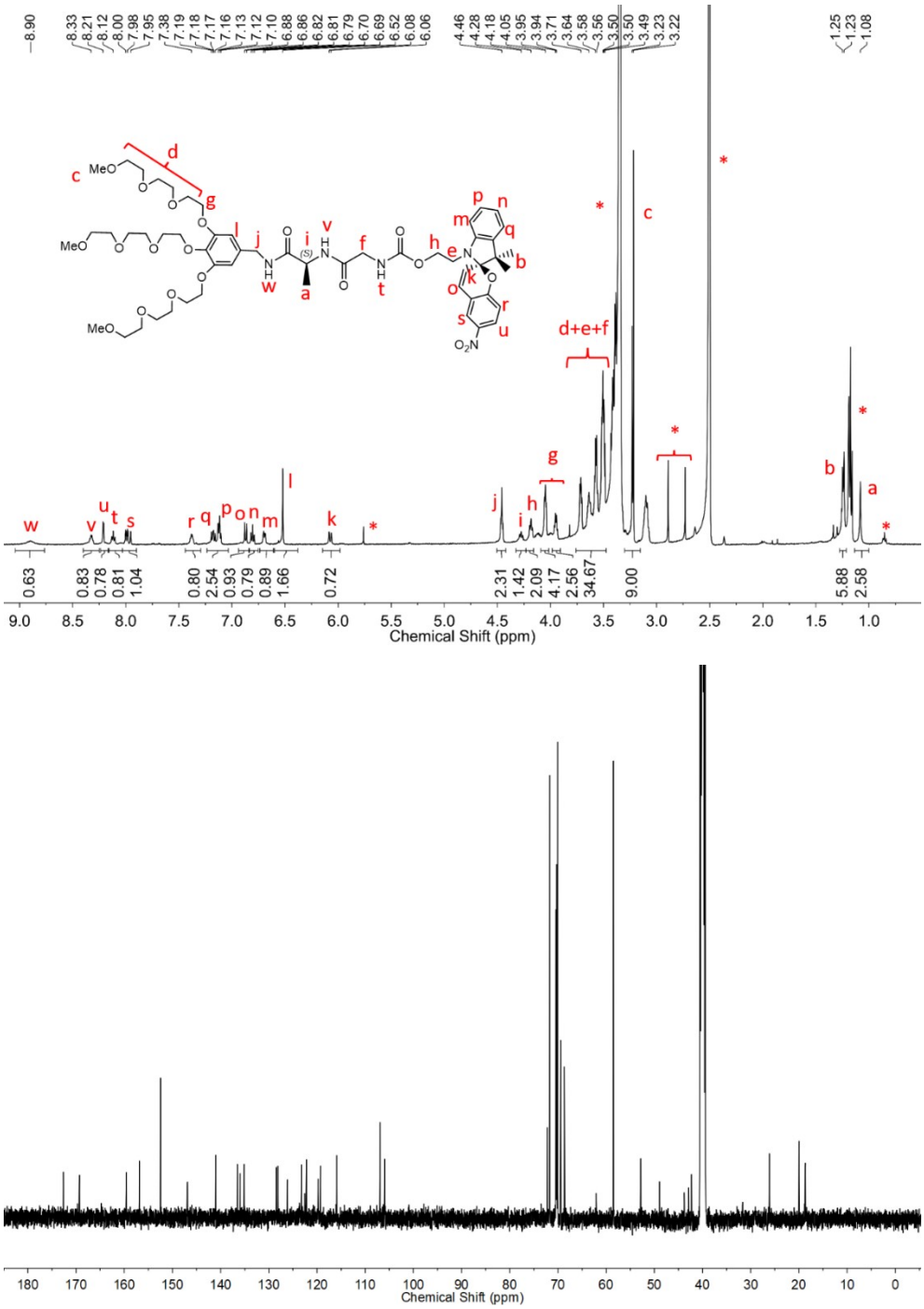

Fig. S3 ^{1}H and ^{13}C NMR spectrum of compound **SP-GA-MeG1** in DMSO-d_6 at 295 K.

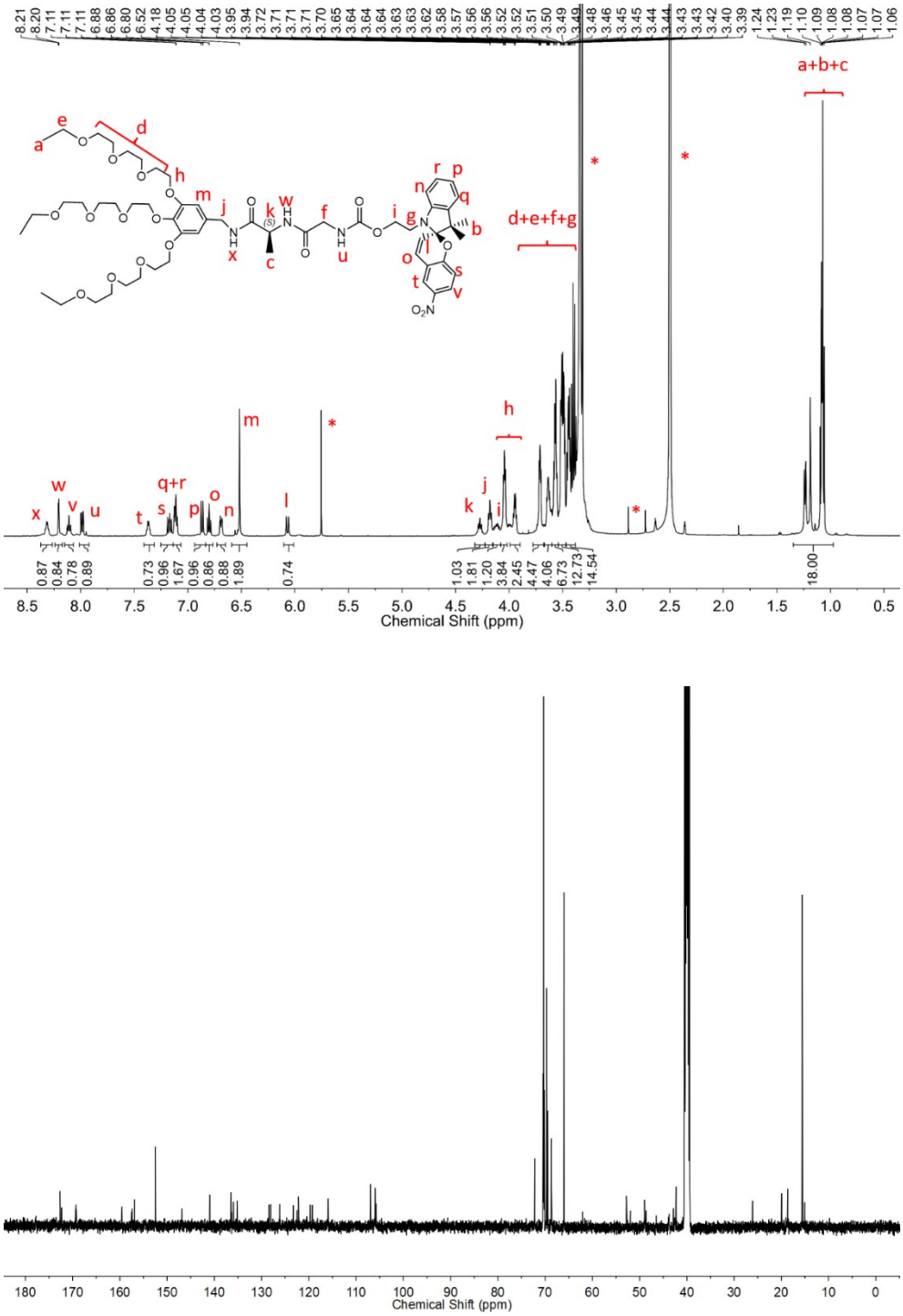

Fig. S4 ^{1}H and ^{13}C NMR spectrum of compound **SP-GA-EtG1** in DMSO-d_6 at 295 K.

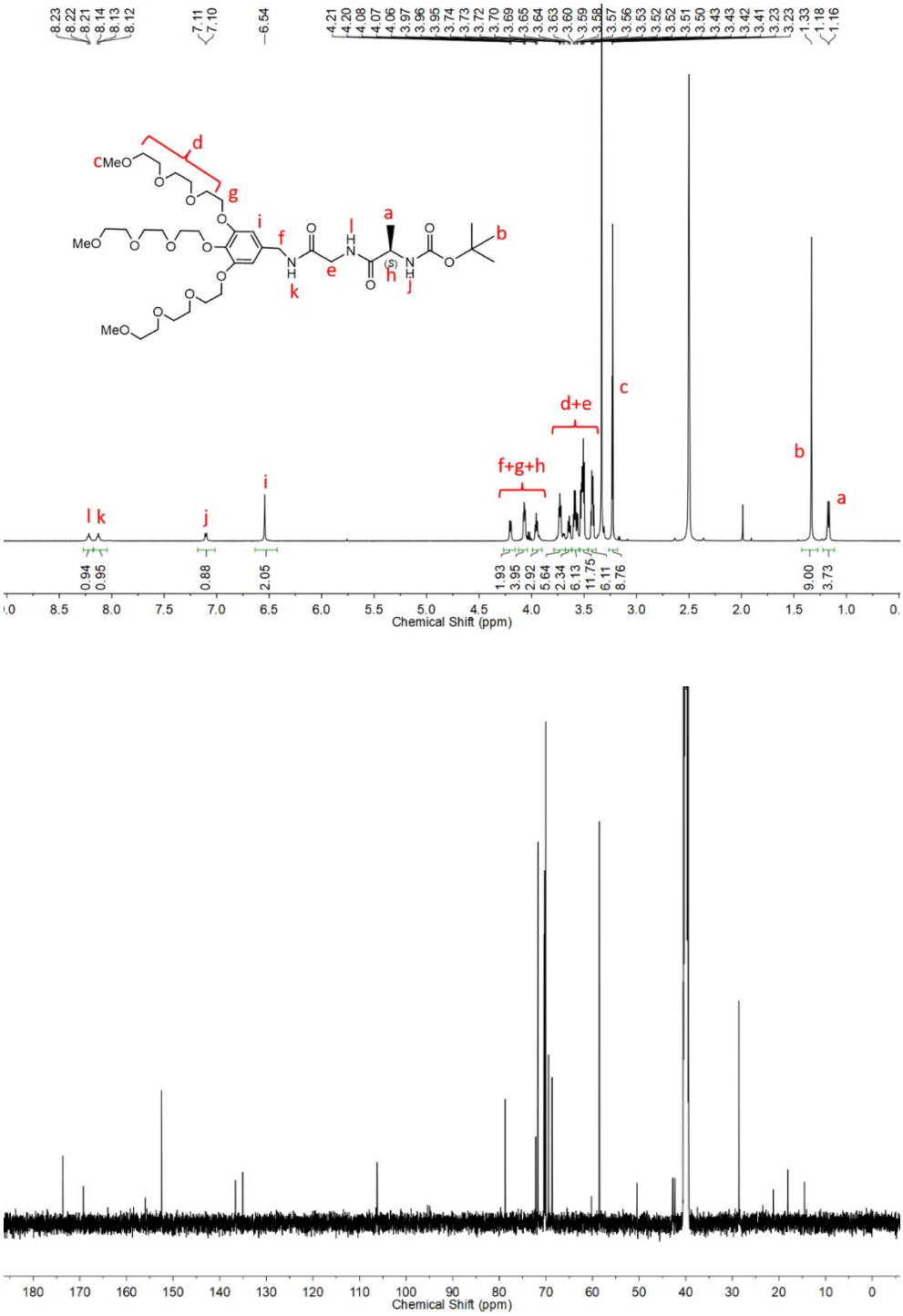

Fig. S5 ^{1}H and ^{13}C NMR spectrum of compound **3a** in DMSO-d_6 at 295 K.

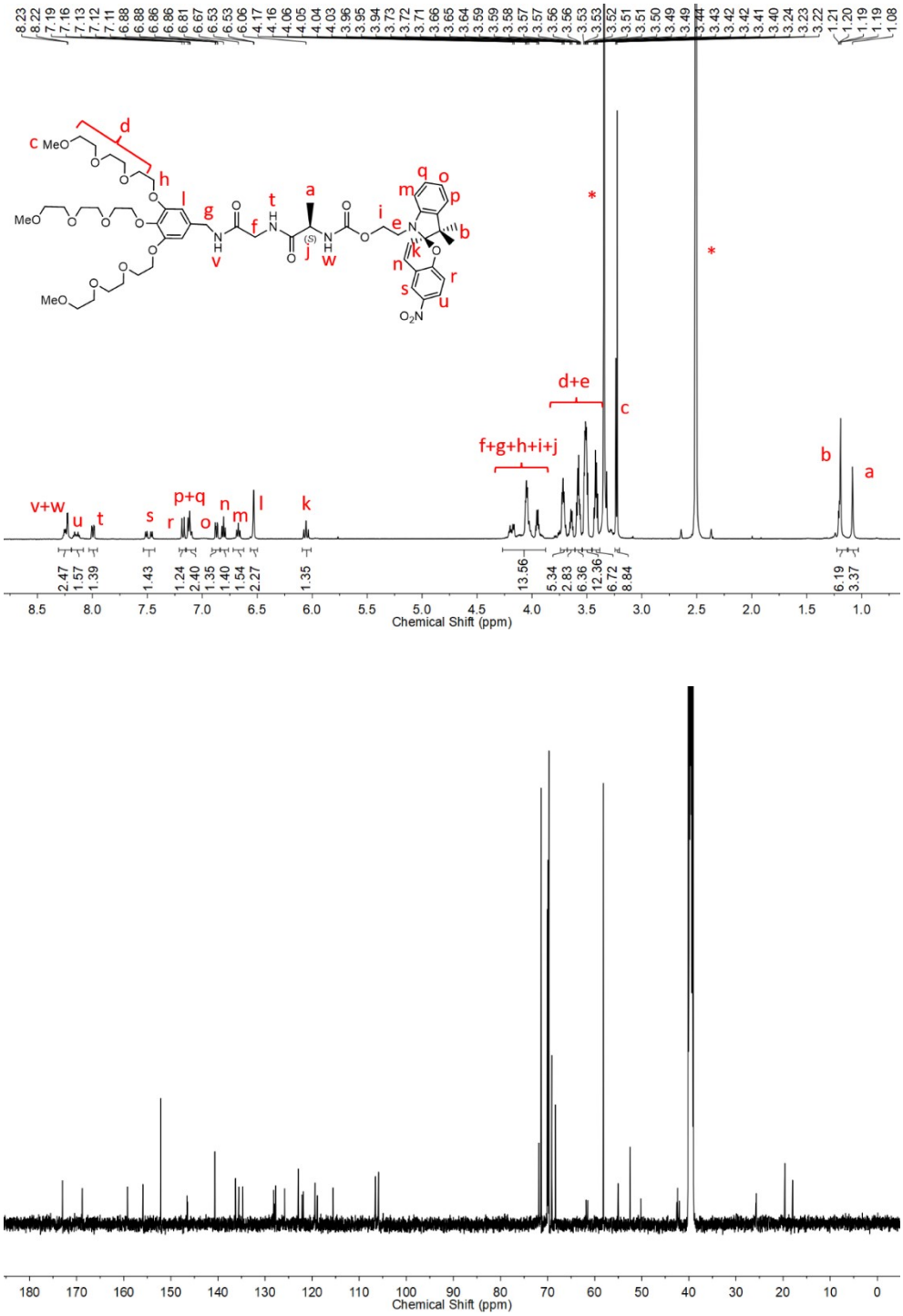

Fig. S6 ^{1}H and ^{13}C NMR spectrum of compound **SP-AG-MeG1** in DMSO-d_6 at 295 K.

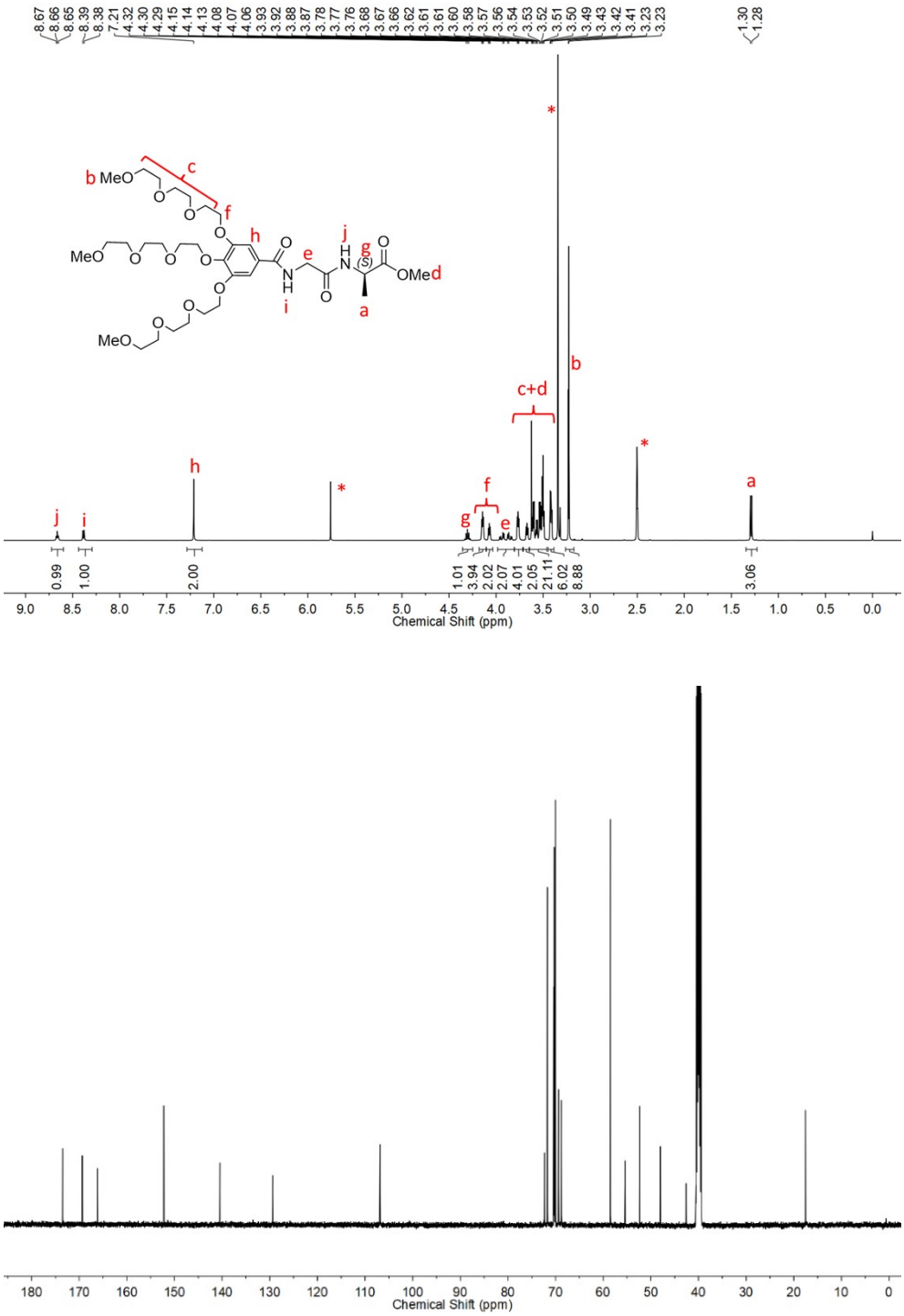

Fig. S7 ^{1}H and ^{13}C NMR spectrum of compound **4a** in DMSO-d_6 at 295 K.

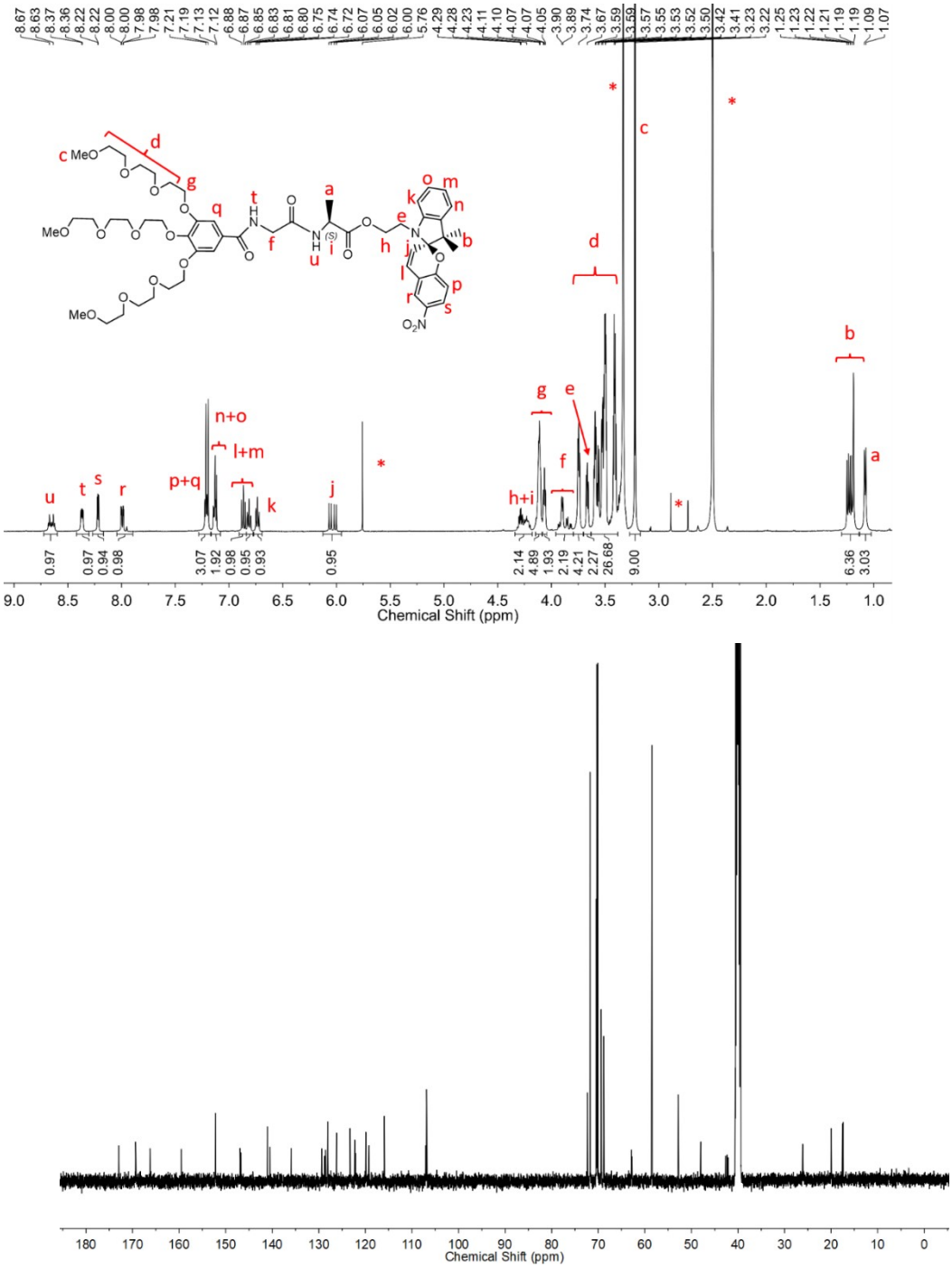

Fig. S8 ^{1}H and ^{13}C NMR spectrum of compound **MeG1-GA-SP** in DMSO-d_6 at 295 K.

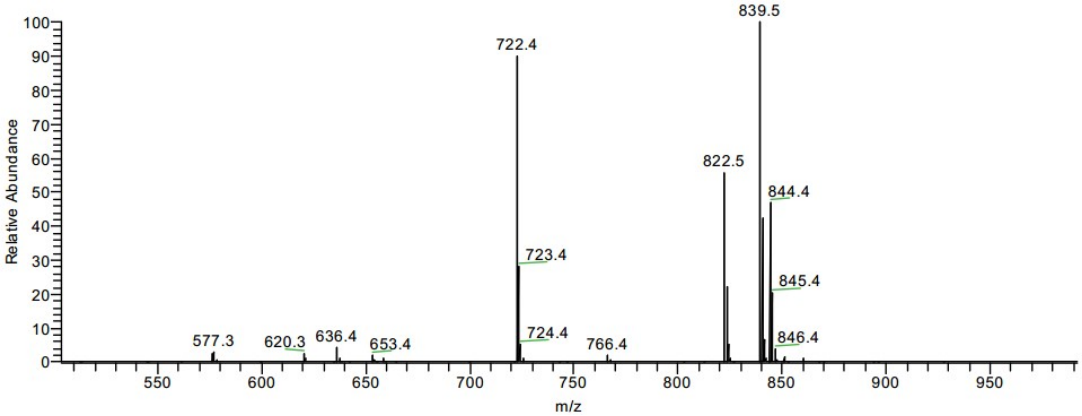

Fig. S9 ESI-MS spectrum of compound **2a** (pos. mode, THF).

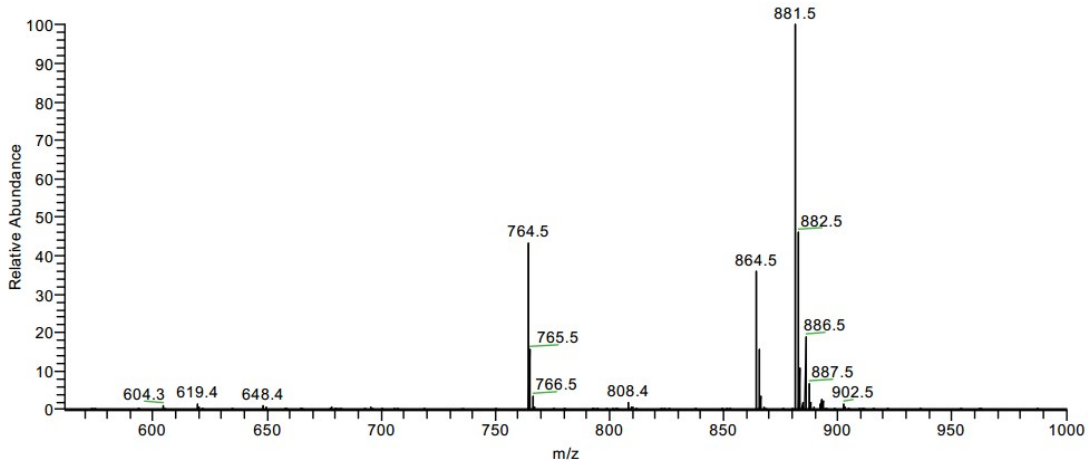

Fig. S10 ESI-MS spectrum of compound **2c** (pos. mode, DCM).

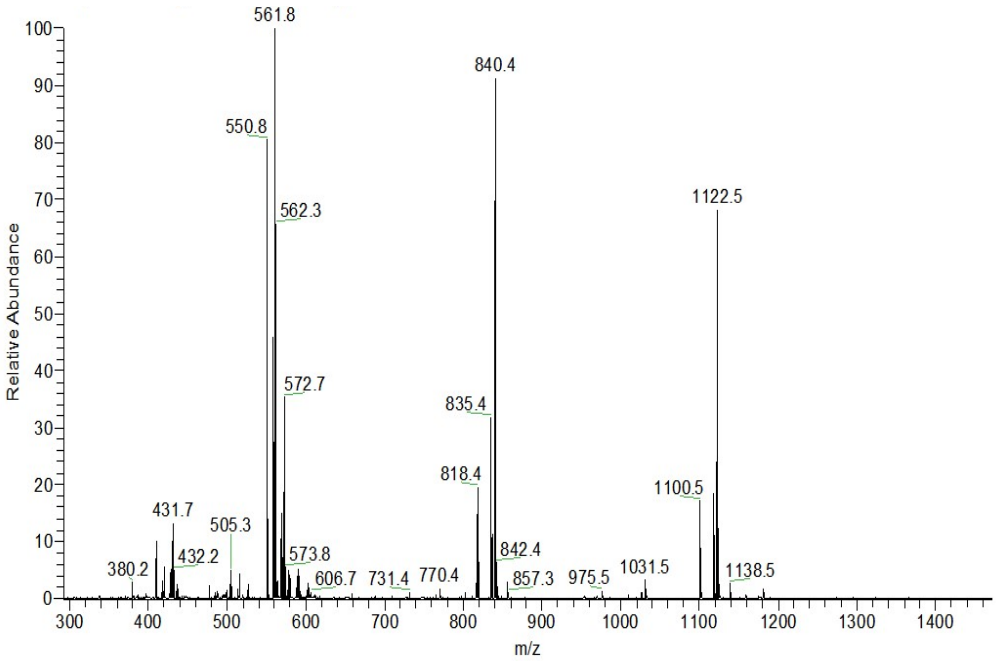

Fig. S11 ESI-MS spectrum of compound **SP-GA-MeG1** (pos. mode, DCM).

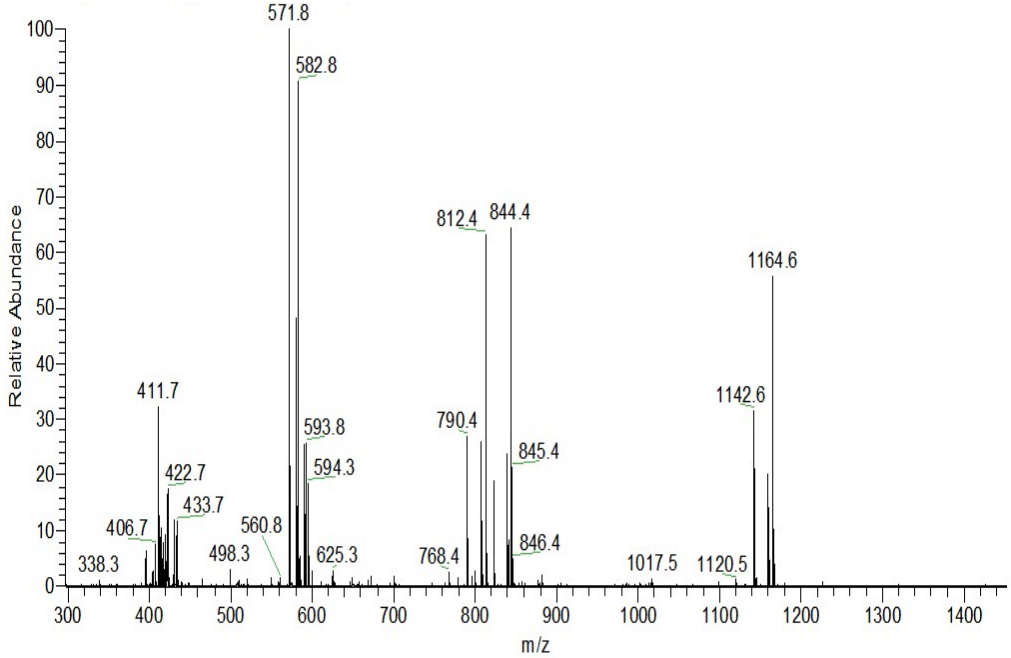

Fig. S12 ESI-MS spectrum of compound **SP-GA-EtG1** (pos. mode, DCM).

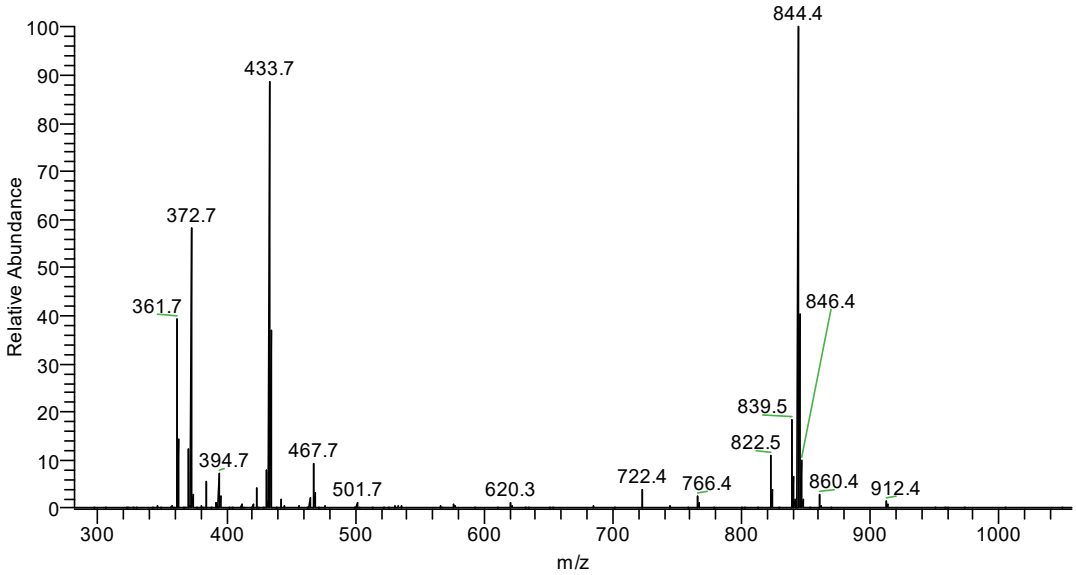

Fig. S13 ESI-MS spectrum of compound **3a** (pos. mode, DCM).

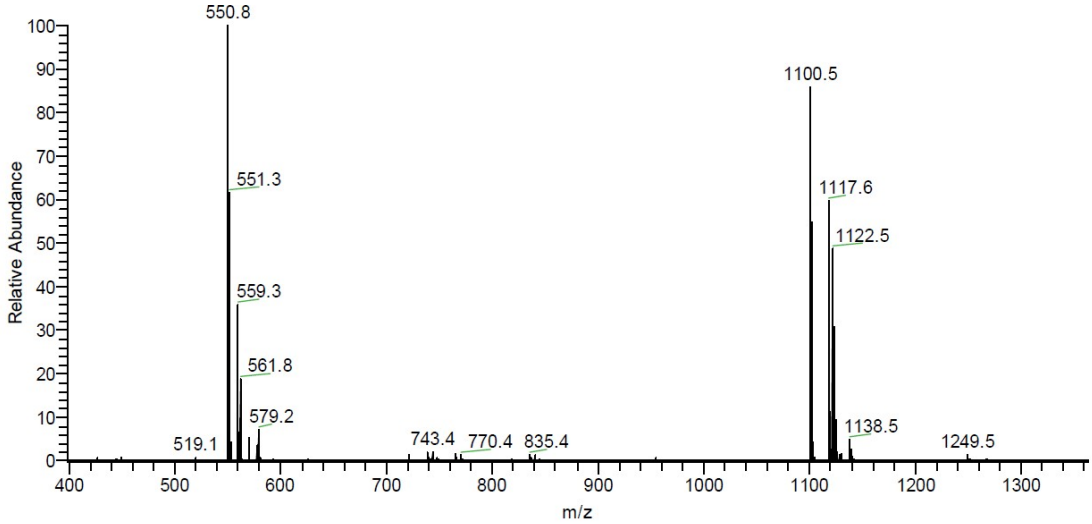

Fig. S14 ESI-MS spectrum of compound **SP-AG-MeG1** (pos. mode, DCM).

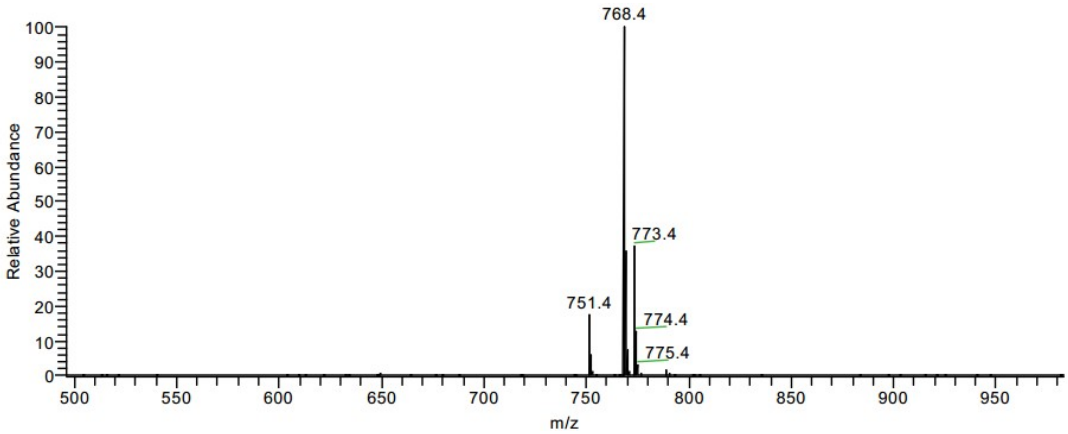

Fig. S15 ESI-MS spectrum of compound **4a** (pos. mode, DCM).

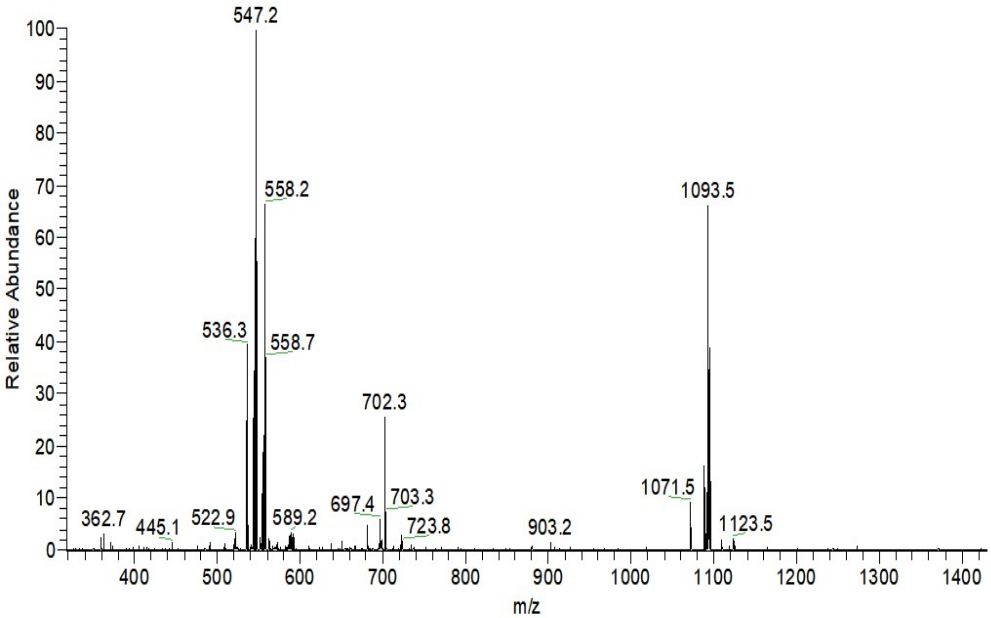

Fig. S16 ESI-MS spectrum of compound **MeG1-GA-SP** (pos. mode, DCM).

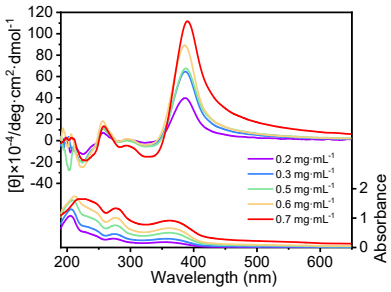

Fig. 17 CD spectra of **SP-GA-MeG1** in aqueous solutions with different concentration at 10 °C.

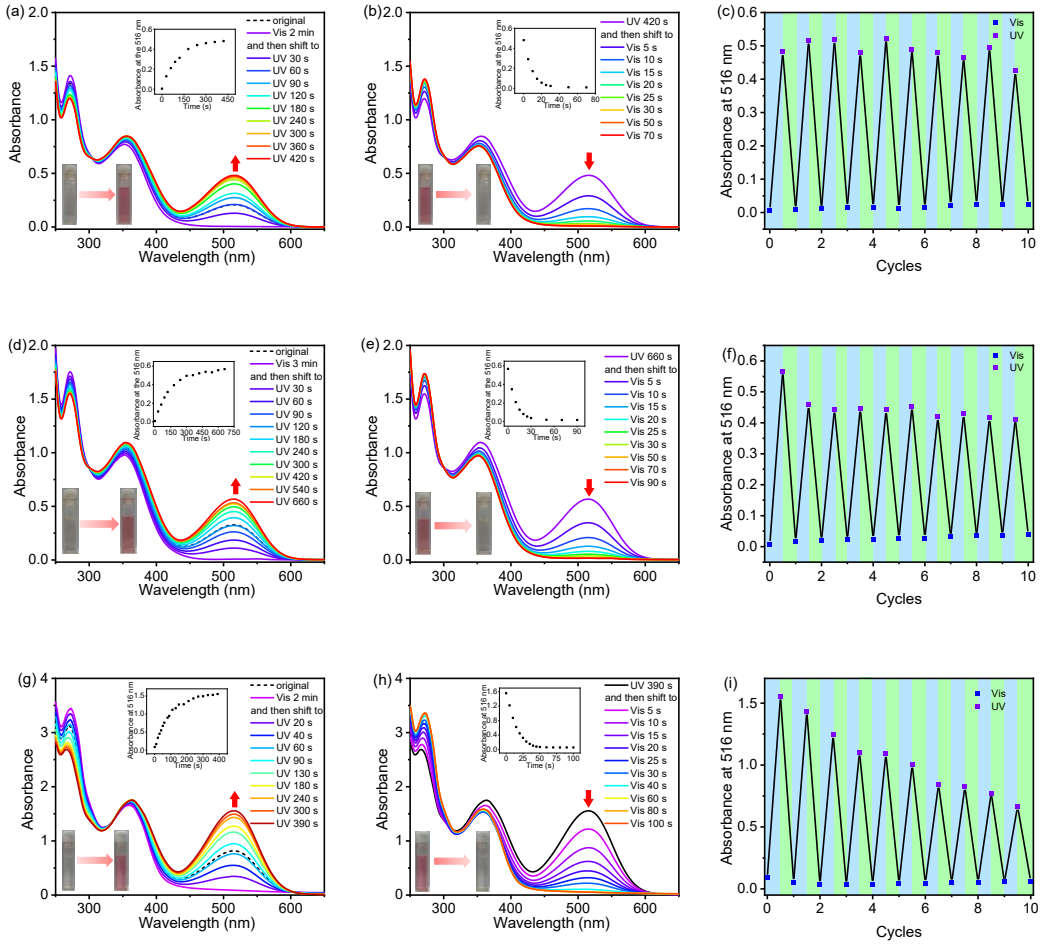

Fig. S18 UV/vis spectra in water of **SP-GA-EtG1** after irradiation with UV (a) and re-irradiation with visible light (b), of **SP-AG-MeG1** after irradiation with UV (d) and re-irradiation with visible light (e) and of **MeG1-GA-SP** after irradiation with UV (g) and re-irradiation with visible light (h), as well as absorbance at 516 nm after alternative irradiation with UV and visible light for **SP-GA-EtG1** (c), **SP-AG-MeG1** (f), **MeG1-GA-SP** (i). Insets in (a), (b), (d), (e), (g) and (h): plots of abs at around 516 nm against irradiation time. λ_{UV} = 254 nm; λ_{Vis} > 450 nm; T = 10 °C, C = 0.15 mg·mL^{-1}.

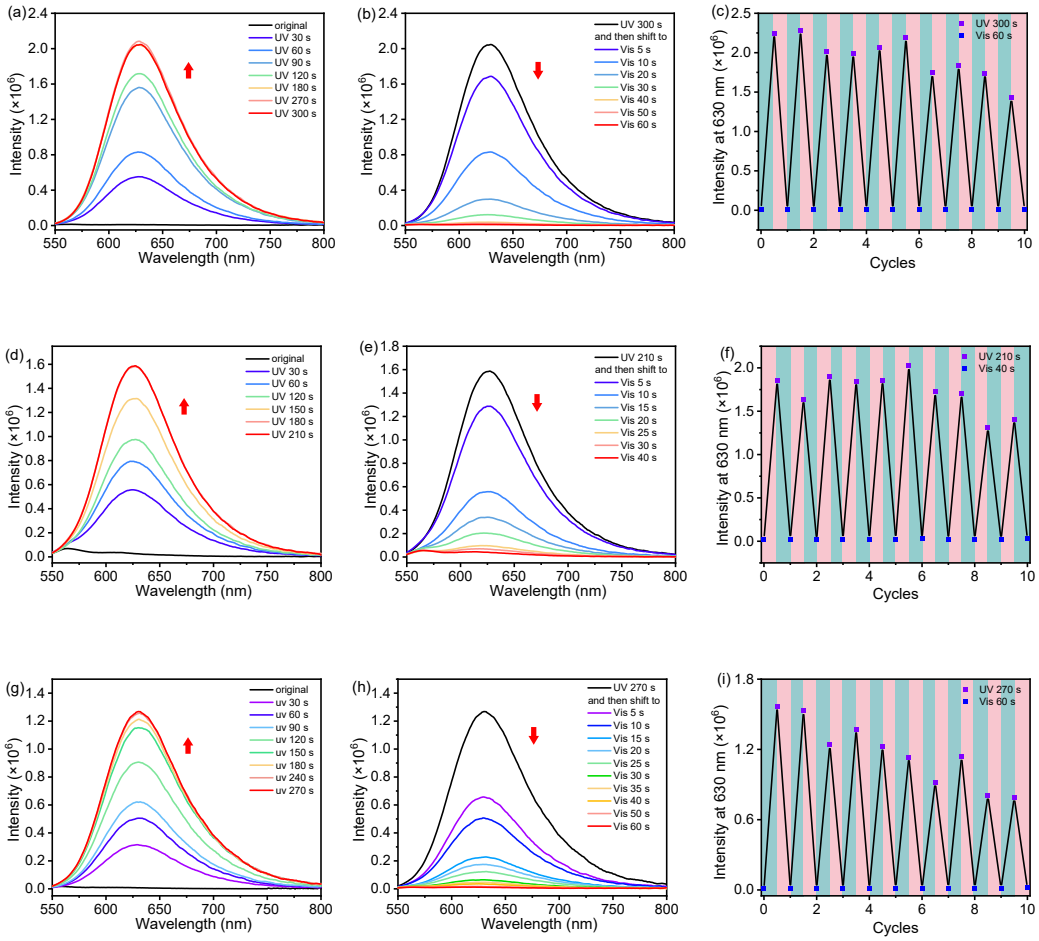

Fig. S19 Fluorescence spectra in water of **SP-GA-EtG1** after irradiation with UV (a) and re-irradiation with visible light (b), of **SP-AG-MeG1** after irradiation with UV (d) and re-irradiation with visible light (e), and of **MeG1-GA-SP** after irradiation with UV (g) and re-irradiation with visible light (h), as well as fluorescence intensity at 630 nm after alternative irradiation with UV and visible light for **SP-GA-EtG1** (c), **SP-AG-MeG1** (f), and **MeG1-GA-SP** (i). λ_{ex} = 535 nm, λ_{UV} = 254 nm, λ_{Vis} > 450 nm, T = 10 °C, C = 0.15 mg·mL^{-1}.

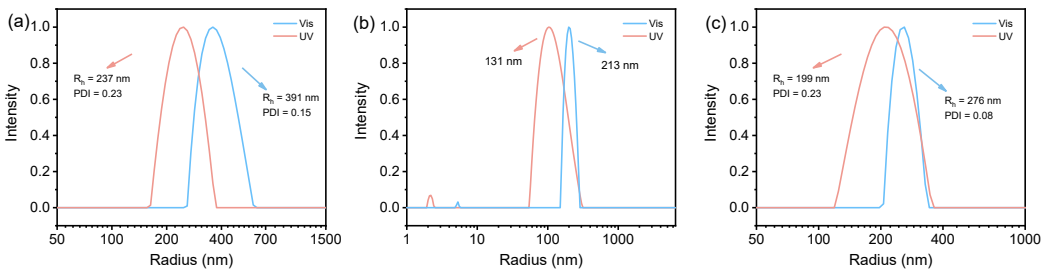

Fig. S20 Plots of hydrodynamic radius of **SP-GA-EtG1** (a), **SP-AG-MeG1** (b), and **MeG1-GA-SP** (c) after irradiation with UV and visible light. λ_{UV} = 254 nm; λ_{Vis} > 450 nm; T = 10 °C, C = 0.15 mg·mL^{-1}.

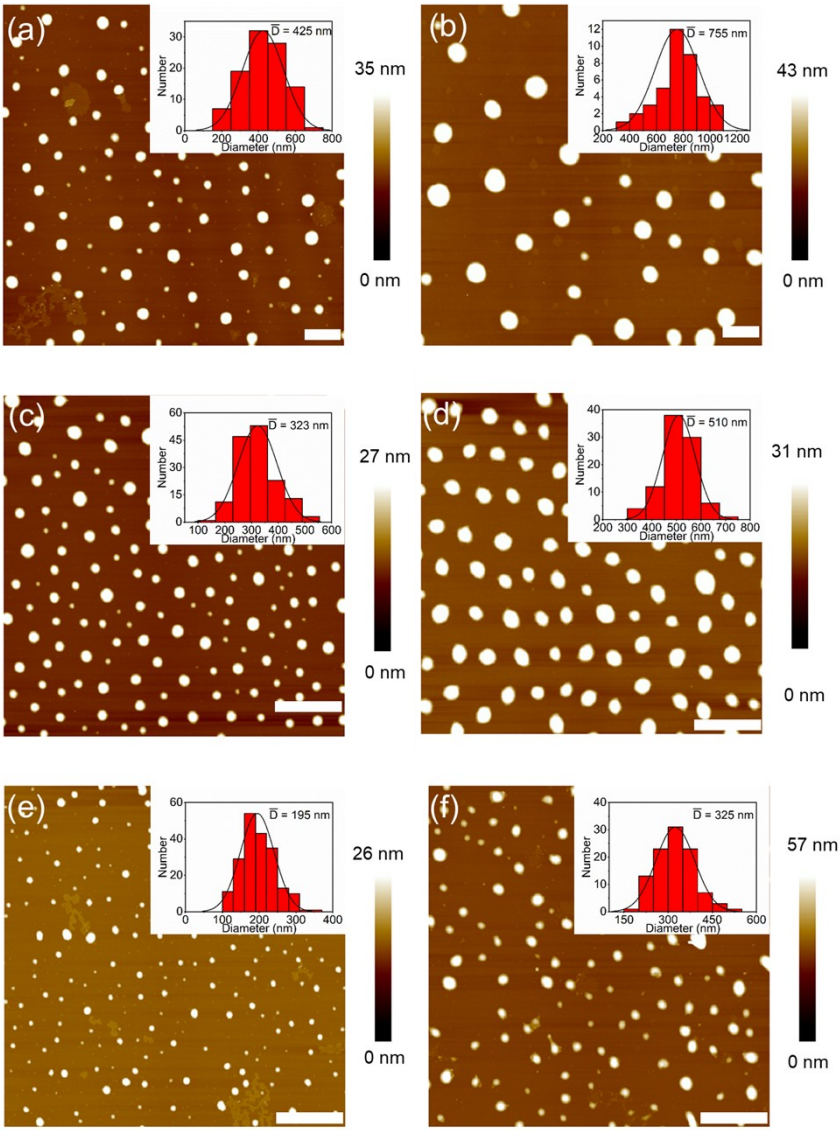

Fig. S21 AFM images of **SP-GA-EtG1** after irradiation with UV (a) and visible light (b), **SP-AG-MeG1** after irradiation with UV (c) and visible light (d), as well as **MeG1-GA-SP** after irradiation with UV (e) and visible light (f). λ_{UV} = 254 nm; λ_{Vis} > 450 nm; T = 10 °C, C = 0.15 mg·mL^{-1}, scale bar = 2 um.

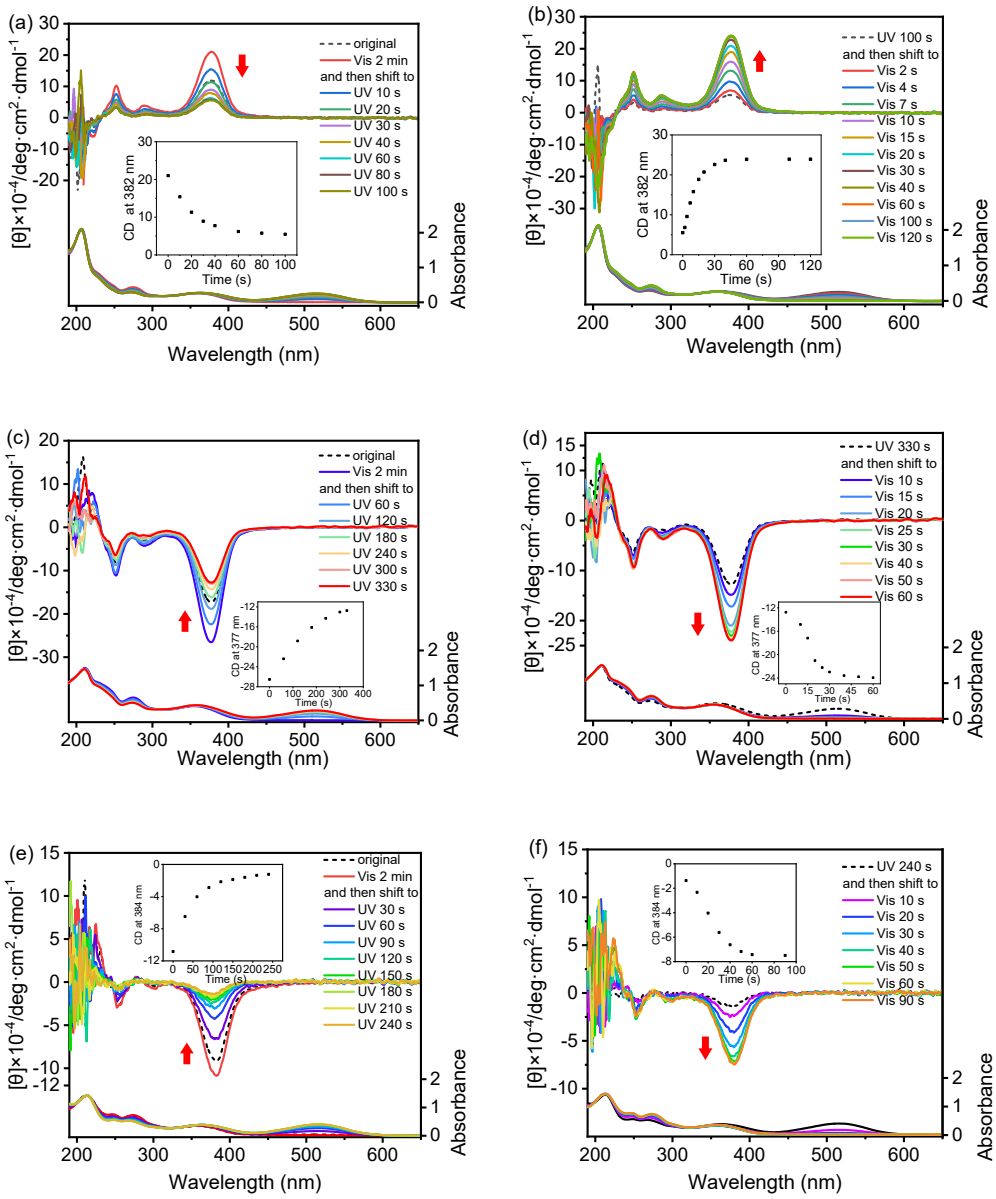

Fig. S22 CD and UV/vis spectra in aqueous solutions of **SP-GA-EtG1** irradiated by UV (a) and re-irradiation with visible light (b), of **SP-AG-MeG1** irradiated by UV (c) and re-irradiation with visible light (d), as well as **MeG1-GA-SP** irradiated by UV (e) and re-irradiation with visible light (f). Insets in (a), (b), (c), (d), (e) and (f): plots of molar ellipticity at around 380 nm (θ_{380}) against irradiation time. λ_{UV} = 254 nm; λ_{Vis} > 450 nm; T = 10 °C, C = 0.3 mg·mL^{-1}.

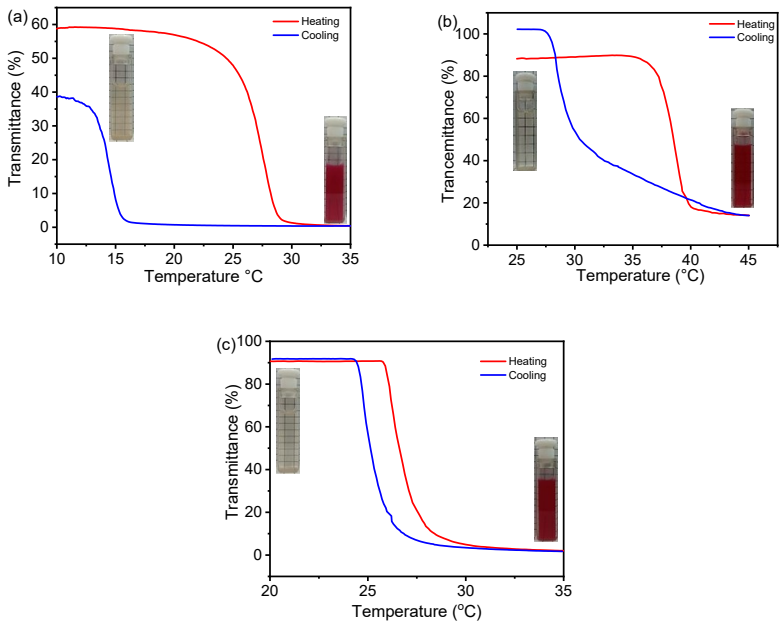

Fig. S23 Plots of transmittance versus temperature for **SP-GA-EtG1** (a), **SP-AG-MeG1** (b) and **MeG1-GA-SP** (c). Heating rate = 0.5 ºC·min^{-1}, C = 0.5 mg·mL^{-1}, wavelength = 700 nm. Inset: photographs of the aqueous solutions below and above their T_{cp}s.

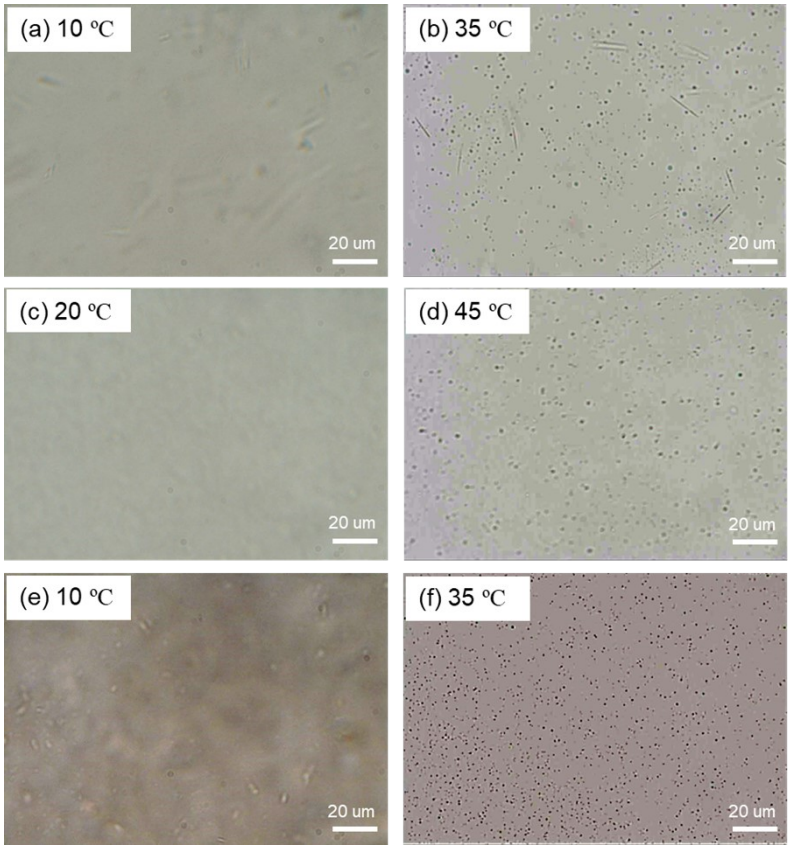

Fig. S24 Microscopic photographs of **SP-GA-EtG1** below (a) and above (b) the T_{cp}, **SP-AG-MeG1** below (c) and above (d) the T_{cp}, as well as **MeG1-GA-SP** below (e) and above (f) the T_{cp}. C = 0.5 mg·mL^{-1}.

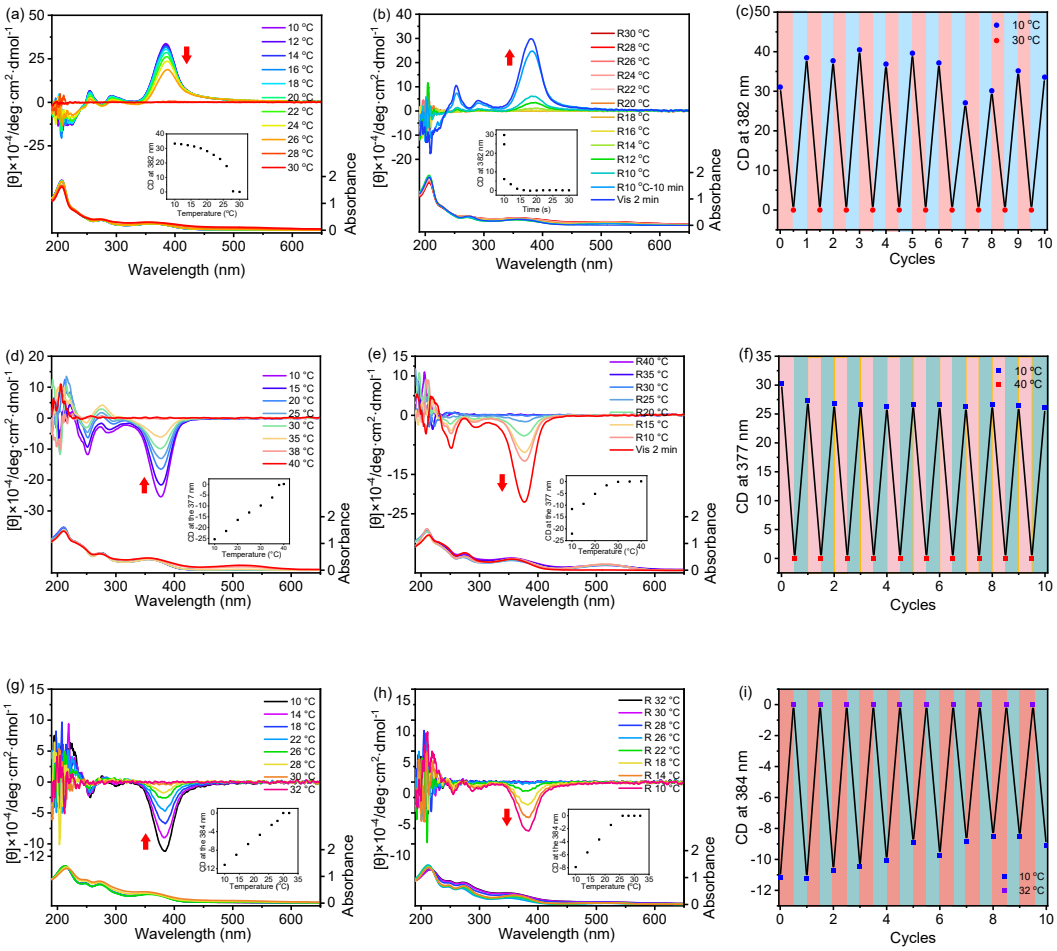

Fig. S25 CD and UV/vis spectra in aqueous solutions of **SP-GA-EtG1** through heating (a) and cooling (b), **SP-AG-MeG1** through heating (d) and cooling (e), **MeG1-GA-SP** through heating (g) and cooling (h), as well as the first Cotton effect at around 380 nm (θ_{380}) after several cycles heating and cooling (through irradiation with visible light): **SP-GA-EtG1** (c), **SP-AG-MeG1** (f), **MeG1-GA-SP** (i). Inset in (a), (b), (d), (e), (g) and (h): plots of molar ellipticity at around 380 nm (θ) against temperature. Heating rate = 2.0 °C·min^{-1}; λ_{Vis} > 450 nm; C = 0.3 mg·mL^{-1}.

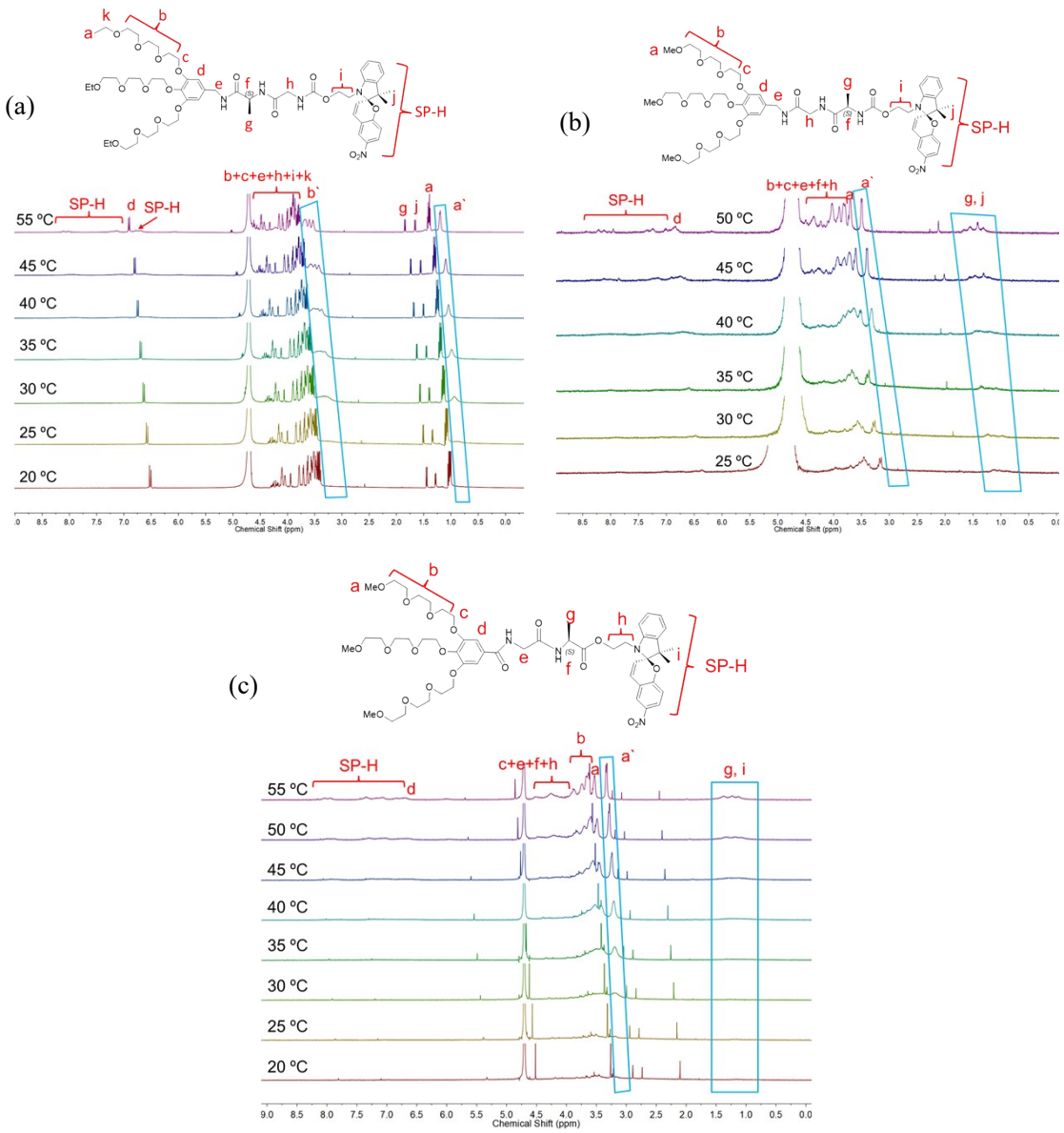

Fig. S26 ^{1}H NMR spectra in D_2O at varied temperatures of **SP-GA-EtG1** (a), **SP-AG-MeG1** (b) and **MeG1-GA-SP** (c). C = 2.5 mg·mL^{-1}.

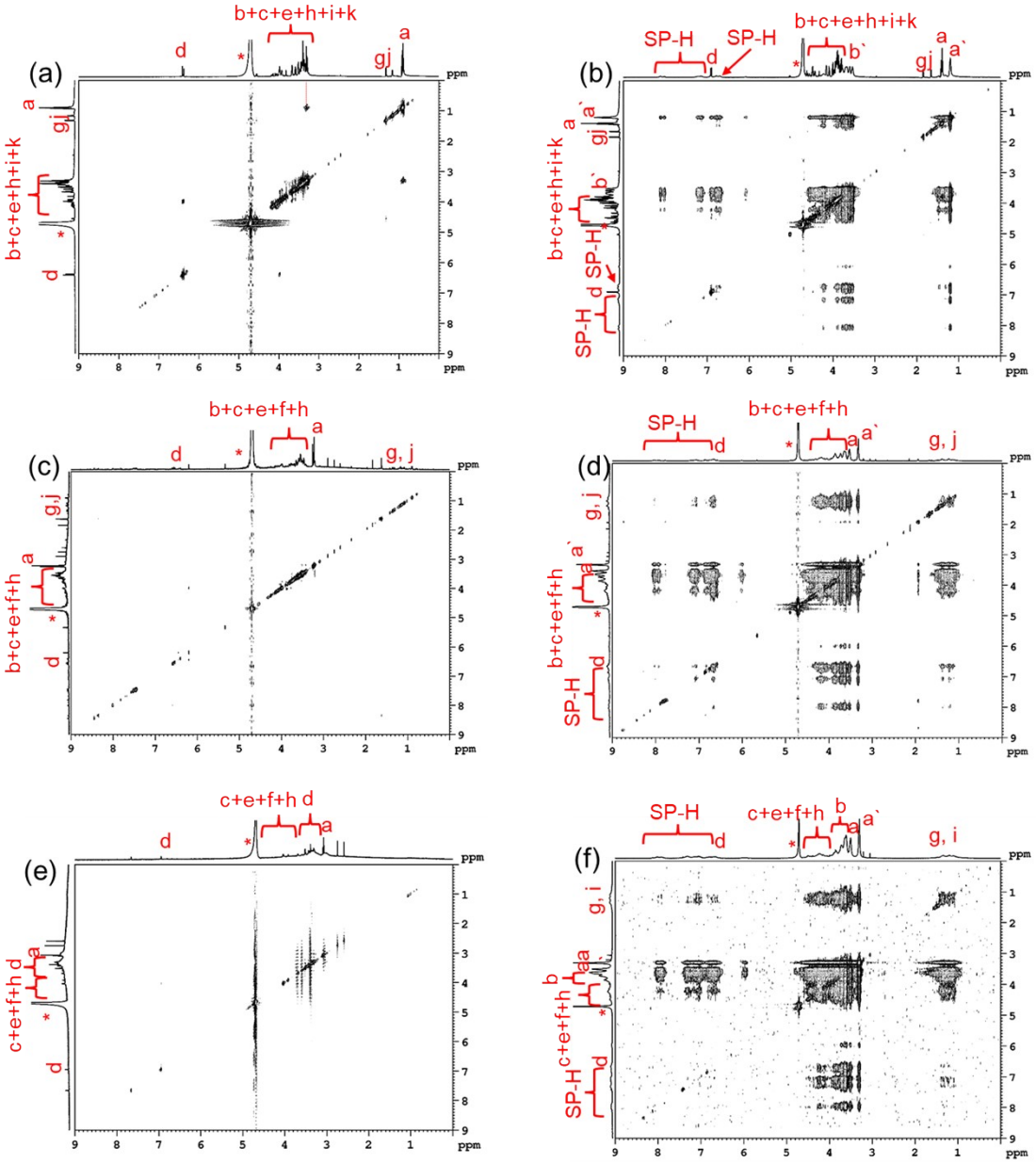

Fig. S27 NOESY spectra of **SP-GA-EtG1** at 10 °C (a) and 55 °C (b), **SP-AG-MeG1** at 10 °C (c) and 50 °C (d), as well as **MeG1-GA-SP** at 10 °C (e) and 50 °C (f). C = 5 mg·mL^{-1}.